Front. Optoelectron. 2016, 9(3): 450–465
DOI 10.1007/s12200-016-0557-8

REVIEW ARTICLE

Asymmetric directional couplers based on silicon nanophotonic waveguides and applications

Daoxin DAI (✉), Shipeng WANG

State Key Laboratory for Modern Optical Instrumentation, Centre for Optical and Electromagnetic Research, Zhejiang Provincial Key Laboratory for Sensing Technologies, Zhejiang University, Hangzhou 310058, China

Abstract Directional couplers (DCs) have been playing an important role as a basic element for realizing power exchange. Previously most work was focused on symmetric DCs and little work was reported for asymmetric directional couplers (ADCs). In recently years, silicon nanophotonic waveguides with ultra-high index contrast and ultra-small cross section have been developed very well and it has been shown that ADCs based on silicon-on-insulator (SOI) nanophotonic waveguides have some unique ability for polarization-selective coupling as well as mode-selective coupling, which are respectively very important for polarization-related systems and mode-division-mulitplexing systems. In this paper, a review is given for the recent progresses on silicon-based ADCs and the applications for power splitting, polarization beam splitting, as well as mode conversion/(de)multiplexing.

Keywords silicon photonics, asymmetric directional couplers (ADCs), polarization-division multiplexing (PDM), mode-division multiplexing (MDM), polarization beam splitter (PBSs)

1 Introduction

A directional coupler (DC) is one of the most important fundamental elements for photonic integrated circuits (PICs) and has been used very widely for power splitting in many photonic integrated devices, including Mach-Zehnder Interferometers (MZIs), microring-resonators (MRRs), etc. DCs can also be used as polarization splitters [1], coarse wavelength-division-multiplexers [2], etc. Because of their extreme importance, lots of papers have been published on the theory, modeling, simulation, and analyses for DCs since integrated optics was proposed in 1960s [3]. A systematic design rules for DCs have been established. Particularly, the coupled mode theory had been developed very well even at the first decade of integrated optics [4]. With the help of coupled mode theory, one can easily calculate the mode coupling in a DC for designing power splitters, wavelength-division-demultiplexers, etc. On the other hand, one should note that most work in the past decades was focused on low-Δ (index-contrast) optical waveguides, e.g., SiO_2-on-Si buried optical waveguides, Ti:$LiNbO_3$ diffusion optical waveguides, etc, which were used as the most popular options previously. For DCs, most of the previous work is focused on the symmetric design consisting of two identical optical waveguides, in which case light power can be transferred from one waveguide to the other one completely when choosing the length L of the coupling region appropriately. And the power coupling ratio can be adjusted between 0 and 100% arbitrarily by modifying the length L, which is very useful for power splitting.

In contrast, an asymmetric directional coupler (ADC) consists of non-identical waveguides in the coupling region. Since the evanescent coupling in an ADC is usually weak possibly due to the phase mismatching, the application of an ADC is quite limited. A potential application reported for ADCs is to realize an optical switch by tuning the refractive index for one of the coupled waveguides [5–7]. In this way, the fundamental modes of two optical waveguides can satisfy or unsatisfy the phase matching condition and thus the evanescent coupling can be enhanced or depressed. For this application, low-index contrast optical waveguides are usually used [5–7]. In the recent years, submicron silicon-on-insulator (SOI) waveguides have been used widely for ultra-compact CMOS-compatible PICs [8–20]. In this case, the situation becomes very different because of the possibility of large cross-sectional asymmetry, ultra-high birefringence, and large mode discrepancy. As a result, there are some unique characteristics of mode coupling and conversion in these waveguides [21,22], and some novel applications can be explored.

Received November 9, 2015; accepted January 6, 2016

E-mail: dxdai@zju.edu.cn

First, ADC can be used to realize some special power splitters. For example, an ADC with two bent waveguides was used successfully to achieve sufficient coupling for realizing a flat-top optical filter based cascaded microrings as a better option than the conventional multimode interference (MMI) couplers or straight DCs. This will be discussed in Section 2.1.

Second, ADCs have also been attracted a lot attention as an excellent candidate for realizing ultracompact and broadband polarization-beam splitters (PBSs) [23–47]. For the application of PBSs using ADCs, one should make the phase matching condition unsatisfied for one polarization mode so that almost no cross-coupling happens. On the other hand, more importantly the ADC should be designed to make the phase matching condition satisfied for the orthogonal polarization mode and consequently this orthogonal polarization mode is cross-coupled completely when choosing the length of the coupling region carefully. In this way, the two orthogonal polarizations (TE and TM) can be separated within a short length (equal to the beat length of the cross-coupled polarization mode). In order to do so, the optical waveguides should have significantly different birefringence. This can be realized by introducing two different types of optical waveguides to form the ADC [42–47], e.g., by using a nano-slot waveguide [48] or silicon hybrid plasmonic waveguide [49] to work with a SOI nanowire. This will be reviewed in Section 2.2.

Third, an ADC can also be used to realize efficient mode coupling/conversion between two types of optical waveguides, which is beneficial for seamless integration between different types of optical waveguides [50]. Furthermore, according to the coupled mode theory, in principle an efficient mode conversion can be achieved between any eigenmodes of two optical waveguides of an ADC when the phase matching condition is satisfied for the two eigenmodes to be coupled so that it is possible to realize mode-selective coupling, which is useful for mode-division-multiplexing (MDM) optical interconnects [51]. This will be discussed in Section 2.3.

These ADCs can be further integrated with other elements to realize some photonic integrated circuits (PICs), which will be reviewed briefly in Section 3.

In this paper, we give a review and summary for the recent progresses on ADCs based on SOI nanowires with ultra-high Δ and their applications for power splitting, polarization beam splitting, as well as mode conversion/(de)multiplexing.

2 ADCs for different applications

2.1 ADCs for power splitting

Power splitting is a one of the most fundamental application for DCs and has been playing an important role for various photonic integrated devices like MRRs. For MRRs, the coupling ratio is usually chosen according to the requirement for the 3 dB bandwidth. However, the regular DCs might not be a good option for some specific cases, even though it is easy to realize an arbitrary power splitting ratio (or coupling ratio) by choosing the length of the coupling region. For example, when MRRs are used as an optical filter, a box-like filtering response is often desired so that it can tolerate a wavelength shift due to any environmental change. This response for optical filters based on MMRs can be synthesized with multiple rings [52–55]. When using multiple microrings to achieve a box-like filtering response, all the couplers involved should be designed optimally to achieve the coupling coefficients as desired [56]. For example, for the ultra-compact 5th order MRR optical filters demonstrated in Ref. [57], the power coupling ratios κ^2 for all the couplers are chosen as 0.45, 0.09, 0.05, 0.05, 0.09, and 0.45, respectively. In order to achieve the sufficient power coupling coefficient as high as 0.45, one usually has to use the design of race-track resonators with long coupling region or narrow gap w_{gap} in the coupling region. However, a longer coupling region causes a smaller free-spectral range (FSR), which limits the channel number available in wavelength-division-multiplexing (WDM) systems. When choosing a narrow gap (e.g., ~20 nm), the beating length becomes small. However, the fabrication (e.g., the lithography and etching processes) becomes difficult and the coupling ratio is very sensitive to the beating length variation [57]. In order to overcome these issues, MMI couplers were used as the coupler with a power ratio of 45%:55% in Ref. [57]. One should realize that the design with MMI couplers has some disadvantages. First, an MMI coupler usually has a few percent of excess loss due to the non-perfect self-imaging in the multimode section [57], and there is also mode conversion loss between the straight section and the bending section of a microring (particularly when the bending radius is ultrasmall). As a result, some notable excess loss will be introduced for an MRR filter. Second, the power splitting ratio of an MMI coupler is fixed [58] and thus it is not flexible to choose any other power splitting ratios in order to achieve a desired 3 dB bandwidth. Third, the length L_{MMI} of the MMI section is usually several microns (e.g., L_{MMI}= ~3.5 μm [57]), which makes the cavity length increased by $2L_{MMI}$ and thus reduces the FSR. These problems can be solved by using bent DCs, as shown in Fig. 1(a) [59].

With bent couplers (which is a kind of ADC, as shown in Fig. 1(b)), there is no excess loss in theory and the cavity length is the same as a regular microring (which has the minimal bending radius). This bent coupler consists of two parallel bent waveguides in the coupling region, i.e., the bent access waveguide and the microring waveguide, which should be designed to be with different widths (w_1, w_2) according to the phase matching condition [40], $n_{eff1}R_1 = n_{eff2}R_2$, where n_{eff1} and n_{eff2} are the effective indices of the fundamental modes of the two bent

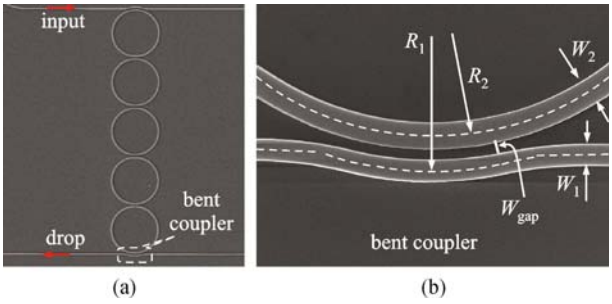

Fig. 1 (a) SEM image of the present five-microring filter with bent couplers; (b) SEM image of the bent coupler used here [59]

waveguides, respectively, R_1 and R_2 are the corresponding bending radii, and $R_1 = R_2 + (w_1 + w_2)/2 + w_{gap}$. The design with the phase matching condition also helps minimize the excitation of higher-order modes in the microring waveguides (which might be multimode). As the coupling ratio can be sufficient as long as the length of the coupling region is long enough, a relatively large gap is allowed ($w_{gap} > 150$ nm) so that the fabrication is not difficult.

As an example, when considering SOI nanowires with a 220 nm-thick top-silicon, the following parameters are chosen as $w_1 = 0.35$ μm, $R_1 = 5.455$ μm, $w_2 = 0.425$ μm, and $R_2 = 4.886$ μm for the bent coupler so that the gap is as large as $w_{gap} = \sim 182$ nm. Figure 2(a) shows the calculated power coupling ratios of the designed bent coupler as the angle θ of the coupling region increases. It can be seen that one obtains the coupling ratio of ~0.45 as required when choosing $\theta = 13.7°$ and the theoretical excess loss of this structure is almost zero in theory. For the inter-ring coupler between two adjacent microrings, the coupling coefficients can be controlled by adjusting the gap between them, as shown in Fig. 2(b). For example, the gap widths are about 116 and 156 nm to achieve the power coupling ratios of 0.09 and 0.05, respectively. It has also been shown that the power coupling ratio for the bent coupler is not sensitive to the deviation Δw, which is an advantage and has been also proposed to realize a broad band 3 dB coupler in Ref. [60] recently. In contrast, the inter-ring coupler is more sensitive to the deviation Δw (see the curves with squares and circles). The spectral response is still box-like even when the deviation Δw is as large as ±20 nm. One should note that the 3 dB bandwidth changes and the ripples increases slightly.

Figures 3(a)–3(b) show the measured spectral responses of the fabricated optical filters with three and five microrings (see the thin curves). The measured responses agree well with the calculated results. Their FSRs are about 18.4 nm and the 3-dB bandwidths are 2.6 and 2.38 nm, respectively. The measured out-of-band rejection ratios for the fabricated three-microring and five-microring filters are about 30 and 36 dB, respectively. It can be seen that higher out-of-band rejection ratio is obtained by introducing more microrings. From the

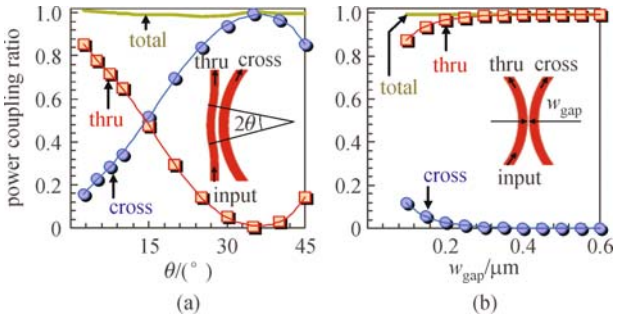

Fig. 2 (a) Simulated power coupling ratio of the bent coupler as the angle θ of the coupling region increases when $w_1 = 0.35$ μm, $R_1 = 5.455$ μm, $w_2 = 0.425$ μm, and $R_2 = 4.886$ μm; (b) coupling ratio of the inter-ring coupler as the gap width w_{gap} varies when choosing $R_2 = 4.886$ μm and $w_2 = 0.425$ μm [59]

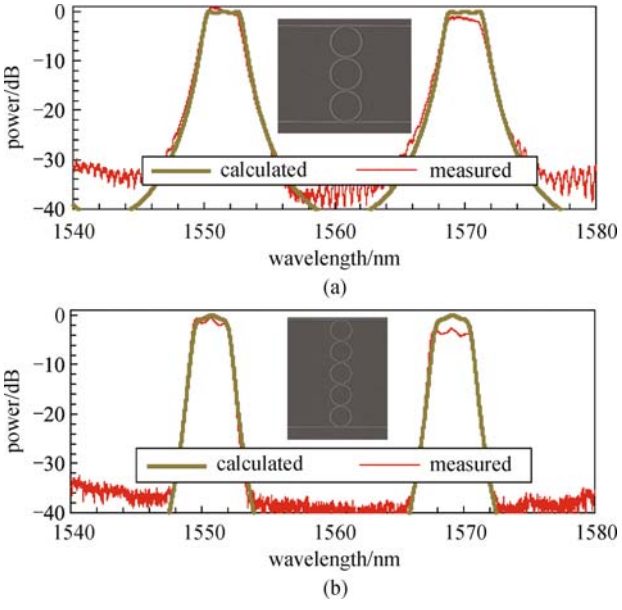

Fig. 3 Measured (thin curves) and simulated (thick curves) responses of the optical filters with (a) three microrings and (b) five microrings. The insets are the SEM images of the filers [59]

measured spectral responses, one can also see that the fabricated three-microring and five-microring filters have an excess loss of < 1.0 dB (@1550 nm), which is beneficial from the low excess loss of the bent couplers in comparison with the MMI couplers or traditional straight-bend coupler used in race-track resonators demonstrated in e.g., Ref. [61].

2.2 ADCs for PBS

A PBS is a basic functional element for many applications when polarization control is needed. Many kinds of on-chip PBSs have been reported by using various structures, e.g., MZIs [26,62], MMI structure [28,29,31], ADCs [1,25,27,32,33,42], and photonic-crystal (PhC)/grating

structures [27,37,38,63]. Among them, an ADC has been proved to be an excellent option for realizing ultra-short PBSs with an ultra-broad band [24]. When designing an ADC to work as a PBS, the waveguide dimension is required to be optimized so that the phase matching condition can be satisfied to have a complete cross-coupling for one polarization only. For the other polarization, the phase matching condition usually is not satisfied due to the strong birefringence of the waveguides, and thus no cross-coupling happens almost. In order to form an ADC, a straightforward way is making the core widths of the two straight optical waveguides in the coupling regions different. However, the phase matching condition won't be satisfied because their fundamental modes are different for any polarization. In the following parts, we give a summary for four types of ADCs used popularly.

2.2.1 ADCs with three waveguides

Figure 4(a) shows the ADC based on three waveguides for

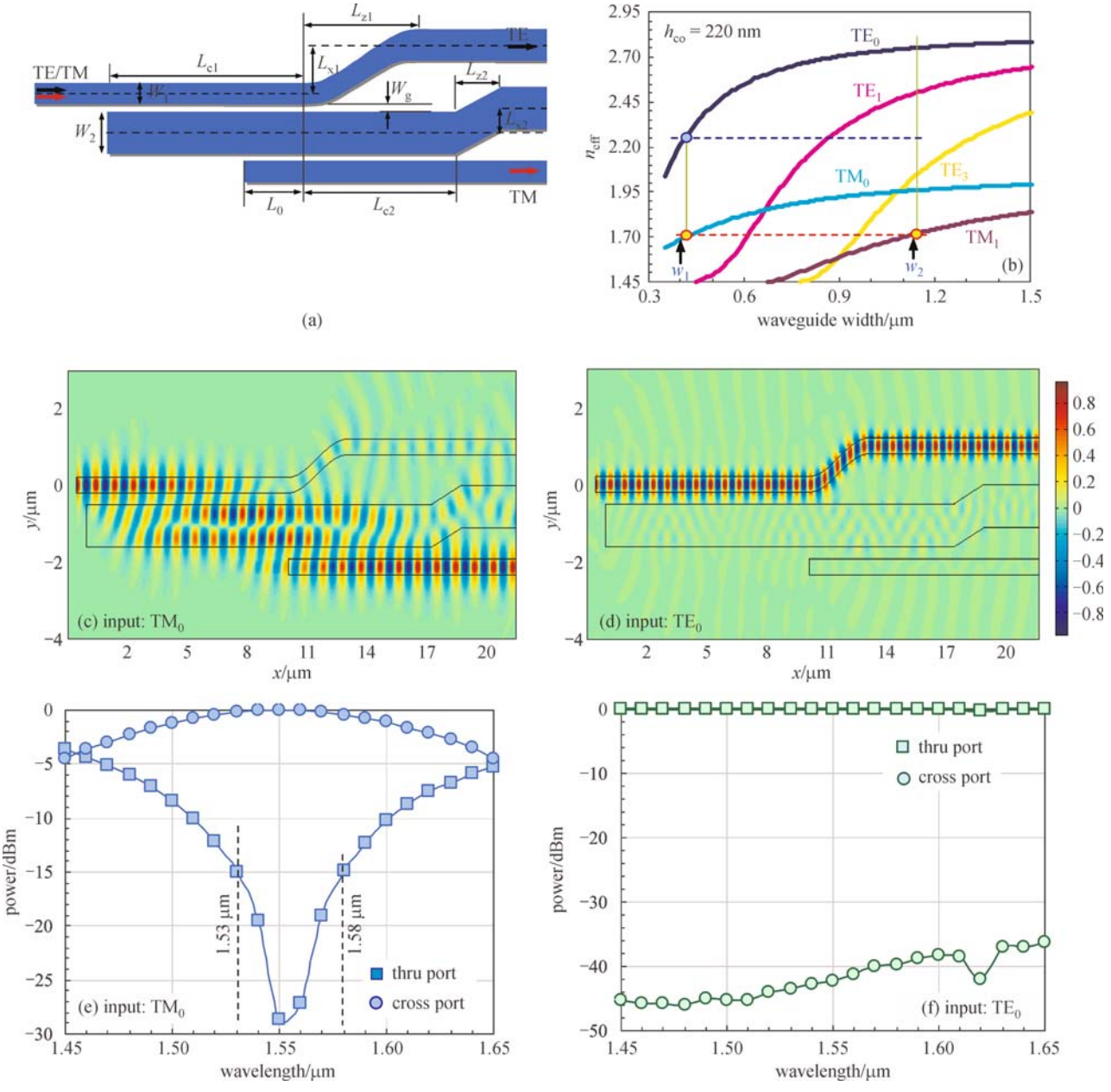

Fig. 4 (a) Schematic configuration of the PBS based on an ADC with three optical waveguides; (b) effective indices of the guided-modes in a SOI nanowire with h_{co}= 220 nm. The simulated light propagation when the light is launched into the PBS (c) for TE polarization and (d) for TM polarization, respectively. The calculated wavelength dependence of the designed PBS when the input is (e) the TM_0 mode, and (f) the TE_0 mode. The parameters are: h_{co}= 220 nm, w_1= 410 nm, w_2= 1.195 μm, w_g= 300 nm, L_{c1}= 11.3 μm, L_{c2}= 12.7 μm, and L_0= –3 μm [39]

realizing a PBS. In this structure, there are two narrow waveguides and a wide waveguide inserted between them. The waveguide widths are chosen optimally so that the phase matching condition is satisfied for TM polarization between the fundamental mode in the narrow optical waveguide and the higher-order mode in the wide optical waveguide (i.e., $n_{\mathrm{eff0(1)}}= n_{\mathrm{eff1(2)}}$) [39], which can be done easily according to the calculated effective indices for all the eigenmodes as shown in Fig. 4(b). Therefore, the TM_0 mode launched at the input port of the narrow waveguide will be cross-coupled to the higher-order mode in the wide waveguide very efficiently when the length of the coupling region is optimized. Another narrow optical waveguide is placed at the other side of the wide optical waveguide so that an output with a fundamental mode is achieved, as shown in Fig. 4(c). From Fig. 4(b), it can be also seen that the phase-matching condition is not satisfied for TE polarization due to the high birefringence of SOI nanowires. As a consequence, when the TE_0 mode is launched, no coupling happens almost, as shown in Fig. 4(d). Figures 4(e)–4(f) show the calculated wavelength dependence of the output powers at the cross port and the through port when the input is the TM_0, and the TE_0 modes, respectively. It can be seen that the output is not sensitive to the wavelength variation when the TE_0 mode is launched and the extinction ratio is higher than 35 dB over a very broad wavelength range from 1.45 to 1.65 μm. In contrast, for the case when the TM_0 mode is input, the response is more sensitive to the wavelength due to the wavelength dependences of the evanescent coupling length. Nevertheless, the designed PBS still has a relatively large bandwidth ranging from 1.53 to 1.58 μm for an extinction ratio of 15 dB.

2.2.2 ADCs with bent waveguides

Figure 5 shows an ADC based on bent waveguides, which consists of two bent waveguides with different core widths. In this structure, the phase matching condition is given by $n_{\mathrm{eff0(1)}}R_1= n_{\mathrm{eff0(2)}}R_2$, where R_1 and R_2 are the bending radii of the narrow and wide optical waveguides. As a result, it is possible to satisfy the phase matching condition for these two bent waveguides with different core widths by choosing the bending radius appropriately. Generally the narrow optical waveguide should have a larger bending radius than the wide optical waveguide (i.e., $R_1 > R_2$) [40]. Figures 6(a) and 6(b) respectively show the calculated optical path lengths (OPL) (with $\theta= 1$ rad and $R_2= 20$ μm) for the TE_0 and TM_0 modes as the waveguide width varies. From Fig. 6(a), one can easily obtain a pair of optimal widths (w_1, and w_2) satisfying the phase matching condition for the TM_0 modes in waveguides #1 and #2. For example, one can choose (w_1, w_2)=(0.534 μm, 0.46 μm) as indicated by the dashed line in Fig. 6(a). On the other hand, for the TE_0 mode, there is a notable phase mismatching when choosing the optimal widths (w_1, w_2), as shown in Fig. 6(b). Figures 6(c) and 6(d) show the simulated light propagation in the designed bent ADC when the input is with the TM_0 and TE_0 modes, respectively. From these figures, it can be seen that the launched TM_0 mode is coupled completely almost from the narrow optical waveguide to the wide optical waveguide while the TE_0 mode propagates along the narrow input waveguide with negligible cross-coupling. Such a polarization-dependent evanescent coupling enables an ultra-short PBS [40,41].

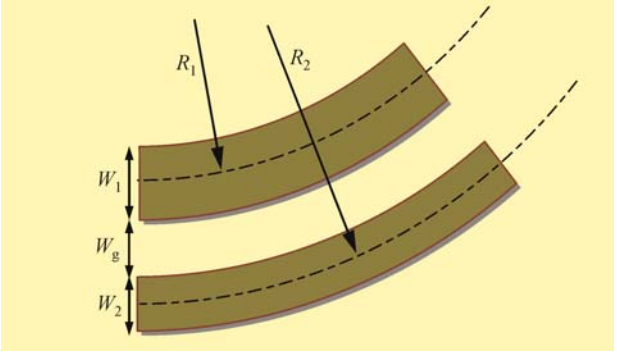

Fig. 5 An bent ADC consisting of two bent waveguides with different core widths [40]

Figures 7(a) and 7(b) respectively show the schematic configuration and the SEM picture for the PBS based on the bent ADC. In order to decouple the two bent waveguides, an S-bend section is cascaded. The S-bend has a sharp bending so that it also works as a TE-passed polarization filter regarding that the TM polarization has a much higher loss than the TE polarization when the bending radius is ultrasmall. Figures 7(c) and 7(d) show the simulated light propagation in the designed PBS for TM and TE polarizations, respectively. It can be seen that the TM polarization is coupled and output from the cross port while the TE polarization is output from the through port with negligible cross-coupling. The total length for the PBS is only 9.5 μm, which is one of the smallest PBS for the case without nanoplasmonic structures involved. Further numerical analyses also show that the present PBS has a very large bandwidth (>200 nm for an extinction ratio of 10 dB) and a large fabrication tolerance ($>\pm60$ nm). Figures 7(e) and 7(f) show the measured transmission responses at the through port and the cross port of the fabricated PBS when TM and TE polarized light are launched respectively. The responses are normalized by the transmission of a straight waveguide. From these figures, it can be seen that the excess losses for both TE and TM polarizations are low at the central wavelength (close to zero). In Figs. 7(e)–7(f), the finite-difference time-domain (FDTD) simulation results for the fabricated PBS are also shown. It can be seen that the simulation and

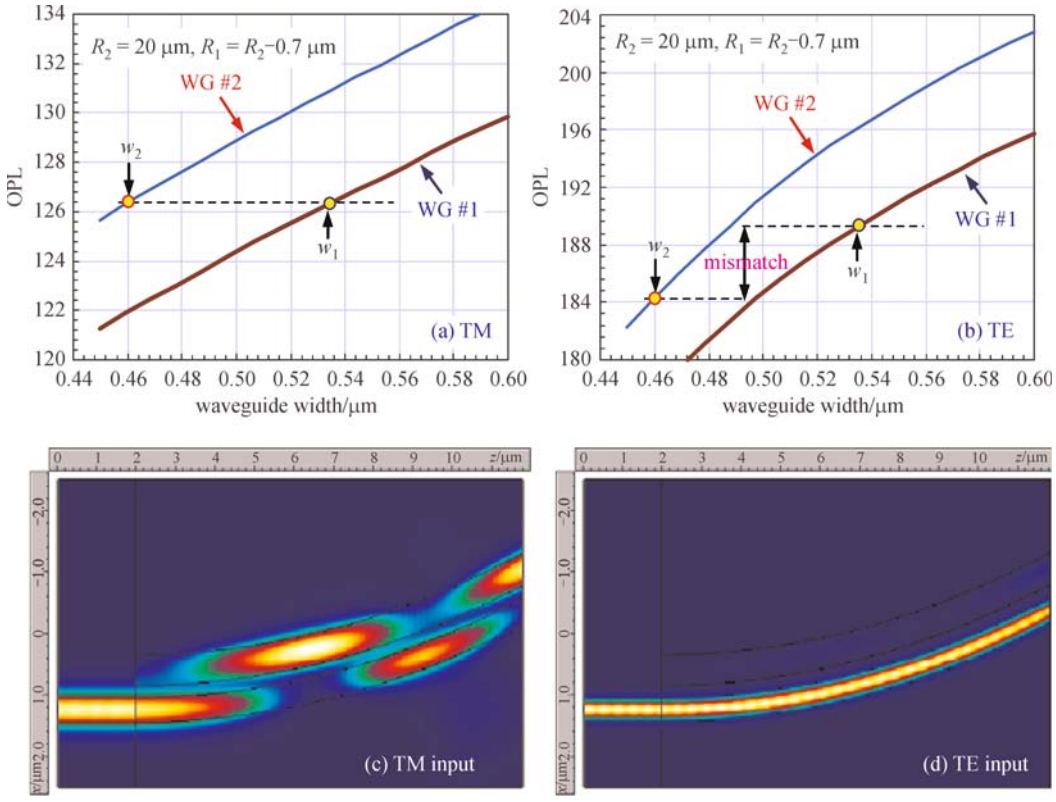

Fig. 6 Optical path lengths (OPL) as the waveguide width varies when R_2= 20 μm: (a) TM, (b) TE; light propagation in the designed bent coupler with R_1= 19.3 μm, R_2= 20.0 μm, w_1= 0.534 μm, w_2= 0.46 μm, and w_g= 203 nm: (c) TM, (d) TE. The SOI wafer has a silicon thickness of h_{co}= 220 nm, and the refractive indices of Si, SiO_2, and air are assumed to be n_{Si}= 3.455, n_{SiO2}= 1.445, and n_{air}= 1.0 respectively [40]

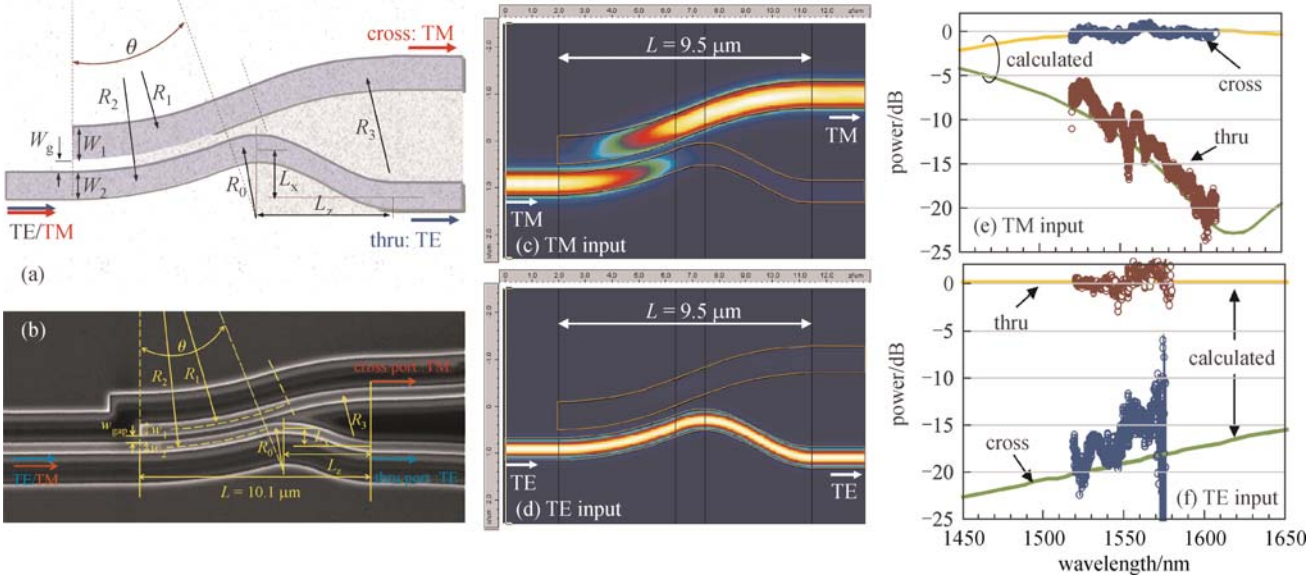

Fig. 7 An ultra-short PBS based on a bent ADC. (a) Schematic configuration; (b) SEM picture. The light propagation in the designed PBS with L_{dc}= 4.5 μm, R_1= 19.3 μm, R_2= 20.0 μm, w_1= 0.534 μm, w_2= 0.46 μm, and w_g= 203 nm: (c) TM, (d) TE. The wavelength dependence of the PBSs: (e) TM, (f) TE [40]

measurement results agree well with each other in the measurement wavelength range. The PBS has a high extinction ratio (ER) (> 15 dB) for TE polarized light in a broad band. In contrast, for the TM polarized light, the response is wavelength-dependent which agrees with the theoretical prediction because of the intrinsic wavelength-

dependence of the evanescent coupling. The ER for TM polarization increases from 6 to 20 dB when the wavelength increases from 1520 to 1600 nm. According to the simulation, one can increase the length of the coupling region appropriately so that the central wavelength (~1620 nm) moves back to the design value (1550 nm). It can be seen that TM polarization has the highest ER (~23 dB) at around 1620 nm. Such an ultra-compact PBS with ultra-broad band and large fabrication tolerance will be useful for many PICs.

2.2.3 ADCs with nano-slot waveguides

An ADC can also be formed by introducing some special optical waveguide, e.g., silicon nano-slot waveguide [48], as shown in Figs. 8(a)–8(b) [42–44]. In the coupling region, these two waveguides are designed according to the phase-matching condition for TM polarization. Figure 8(c) shows the calculated effective indices for the TE- and TM-polarization modes of a SOI nanowire and a nano-slot waveguide as the waveguide core widths (w_{Si}, w_{co}) varies when the core height is chosen as h_{co}= 250 nm. It can be seen that these two different types of waveguides have similar effective indices for the TM polarization mode, and consequently it is easily to make the phase matching condition satisfied (i.e., n_{eff_TM1}= n_{eff_TM2}) by choosing the core width w_{co} and w_{Si} appropriately, e.g., w_{co}= 0.4 μm, w_{Si} = 0.26 μm and w_{slot}= 60 nm. As a result, the TM_0 mode can be coupled completely to the cross port when the length of the coupling region is also chosen appropriately (see Fig. 8(d)). In contrast, there is a significant phase mismatch for the TE polarization mode. Thus the evanescent coupling is negligible possibly, and finally the TE polarized light is then output from the through port (see Fig. 8(d)). In order to minimize the footprint, the mode converter between a SOI nanowire and a nano-slot waveguide is merged with the S-bend. With this mode converter, low-loss connection between a SOI nanowire and a nano-slot waveguide is realized, the present design merges the mode converters between the nano-slot waveguide and the regular SOI nanowire into the S-bends at the side of the nano-slot waveguide, as shown in Fig. 8(a). With such a design, the PBS is as short as 6.9 μm.

2.2.4 ADCs with silicon hybrid plasmonic waveguides

It is well known that the mode behavior in surface plasmon polariton (SPP) nanostructures usually have very strong polarization dependence because SPP effect occurs for the polarization mode whose electrical field is perpendicular to the metal-dielectric interface only. Therefore, using nanoplasmonic waveguides provides a good option for realizing ultra-compact polarization-handling devices. Among various nanoplasmonic waveguides, the hybrid plasmonic waveguides developed recently [49,64–67] are considered as an excellent candidate because it is possible to achieve a nano-scale light confinement as well as relatively long propagation distance simultaneously. In particular, SOI-compatible hybrid plasmonic waveguide shown in Fig. 9(a) [49] is even more attractive because the design and fabrication technologies for silicon photonics can be available compatibly. As shown in Fig. 6(a), a silicon hybrid nanoplasmonic waveguide consists of a SOI nanowire, a metal cap and an ultra-thin SiO_2 layer (h_d) between them. Due to the surface plasmonic effect, a silicon hybrid nanoplasmonic waveguide has very different birefringence from a SOI nanowire. Therefore, it is easy to form an ADC for realizing PBSs by combining a silicon hybrid nanoplasmonics waveguide and SOI nanowires [45–49]. For example, a small PBS is proposed by using an ADC consisting of two SOI nanowires with a silicon hybrid plasmonic waveguide between them

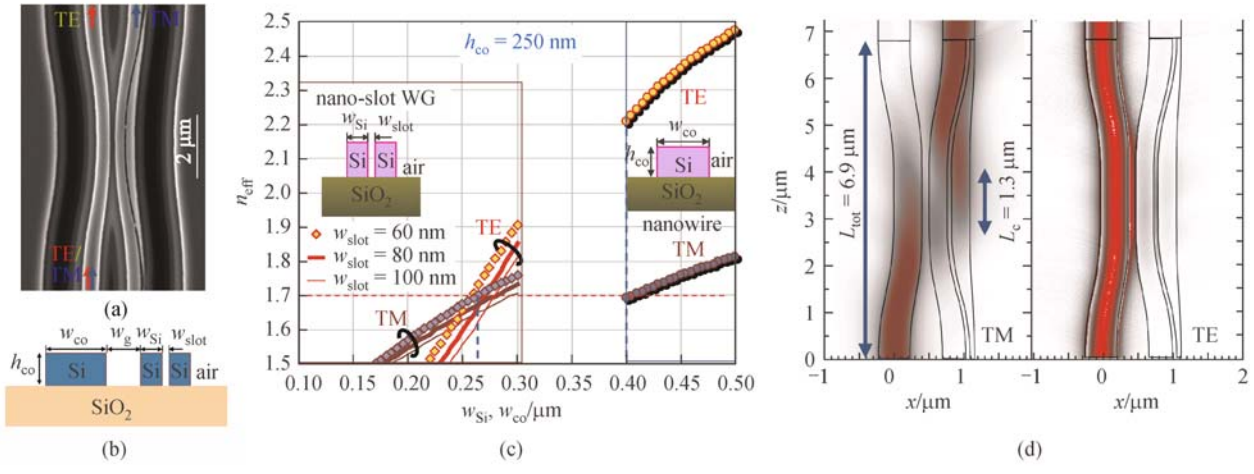

Fig. 8 PBS based on an ADC consisting of a SOI nanowire and a nano-slot waveguide: (a) SEM picture; (b) cross section; (c) calcualted effective indices of a SOI nanowire and a nano-slot waveguide as the core width (w_{Si}, w_{co}) varies; (d) light propagation in the designed PBS with w_{co}= 0.4 μm, w_{Si}= 0.26 μm, h_{co}= 250 nm, w_{slot}= 60 nm, and w_g= 100 nm [43]

[45,46]. The PBS length is about 5 – 10 μm when the waveguides are optimized to make the TM polarization cross-coupled. It is possible to simplify the three-waveguide ADC into an ADC with two waveguides, as shown in Fig. 9(b) [47]. In addition, the waveguides for the ADC can be designed optimally to make the phase-matching condition satisfied for TE polarization (instead of TM polarization in Ref. [47]). In this way, both two waveguides have relatively large widths (w_1, $w_2 \sim 300$ nm) and the length of the coupling region is as short as 2.2 μm even when choosing the gap width as large as $w_{gap} = 200$ nm. Such a relatively large gap makes the fabrication not difficult. Figure 9(d) shows the simulated light propagation in the designed ADC with $L_c = 2.2$ μm and $R = 1.3$ μm when the TE_0 and TM_0 modes are launched. It can be seen that the TE and TM polarizations are separated within the coupling region as short as 2.2 μm and the total length for the PBS is 3.7 μm only.

2.3 ADCs for MDM

MDM is a new technology developed recently to expand the capacity of an optical communication/interconnect link. In order to realize MDM, it is well known that mode multiplexer play an important role as a key component in such a system. In comparison with those mode multiplexers realized with optical fiber couplers [68,69], on-chip mode multiplexers are desired regarding the compactness and the potential to be integrated with other elements on the same chip. Waveguide-grating couplers have been demonstrated to synthesize the desired field profiles and excite a few linearly polarized (LP) fiber modes [70–73]. However, the configuration is quite complicated and the excess loss is relatively large. Recently several kinds of structures for mode (de)multiplexers have been proposed to enable mode multiplexing by using e.g. multimode interferometers [74], adiabatic mode-evolution DCs [75–77], Y-junctions [78–84], as well as ADCs [51,85–91]. Among them, the ADC-based mode (de)multiplexers have the advantages including the broad wavelength band, the ultra-compact footprint and the flexible scalability for more mode channels.

As demonstrated above, an efficient coupling from the TM_0 mode in a narrow input waveguide to the TM_1 mode in a wide middle waveguide was realized with a three-waveguide ADC in Ref. [39]. Similarly, the other higher-order mode in a wide waveguide can also be excited selectively by the fundamental mode in a narrow waveguide. The condition is that the widths (w_a and w_b) of the narrow and wide waveguides should be chosen optimally according to the phase matching condition, i.e., $n_{eff0}(w_a) = n_{effi}(w_b)$, where $n_{eff0}(w_a)$ and $n_{effi}(w_b)$ are the effective indices of the fundamental mode of the narrow access waveguide and the ith higher-order mode of the bus

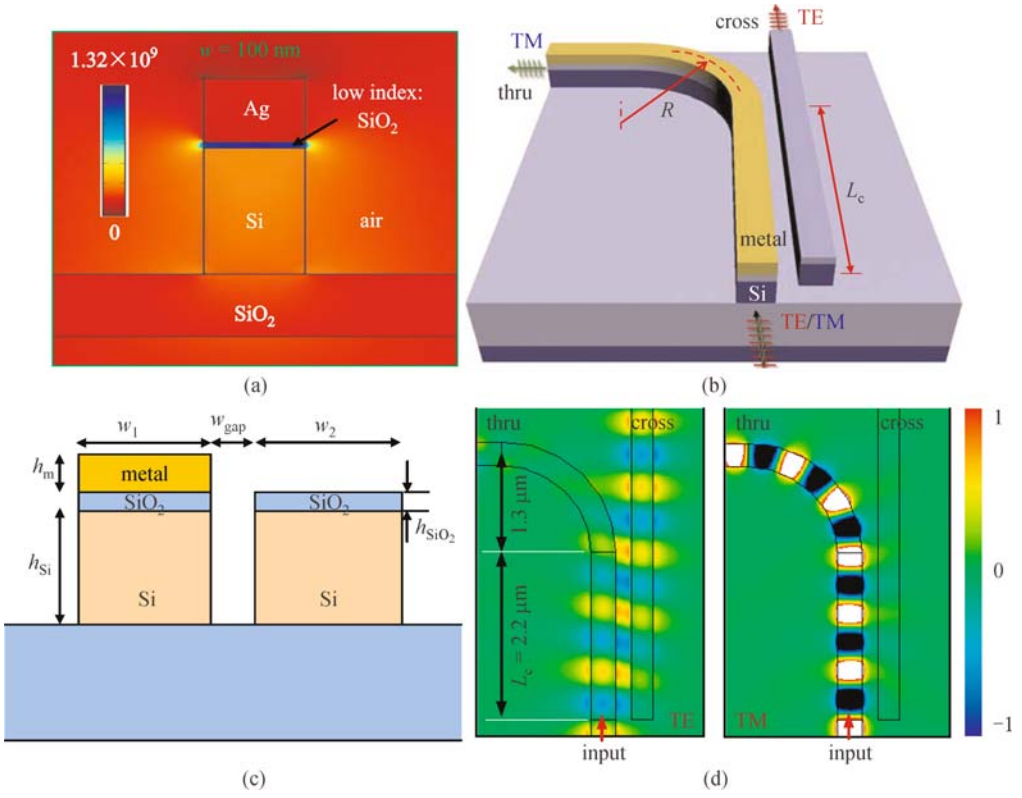

Fig. 9 (a) Cross section of a silicon hybrid plasmonic waveguide with field enhancement in the low index region [49]; (b) schematic configuration of an ADC with a hybrid nanoplasmonic waveguide [47]; (c) cross section of the coupling region of the ADC; (d) 3D-FDTD simulation result for the light propagation in the designed PBS when the input is TE or TM respectively

waveguide, respectively. On the other hand, those undesired eigenmodes will hardly be excited due to the significant phase mismatching. Therefore, one can realize a mode (de)multiplexer with multiple channels [51,86] by cascading ADCs working for different mode-channels. In Refs. [51,86], a 4-channel silicon mode converter-multiplexer with low loss (<0.1 dB), low crosstalk (<-25 dB) as well as small footprint was proposed and demonstrated for the first time. A grating-assist ADC was also designed to construct a 4-channel narrow-band mode converter-multiplexer in Ref. [88]. In Ref. [89], a three-channel converter-multiplexer combining ADCs and microrings for simultaneous mode- and WDM has also been recently realized to expand the link capacity.

As an example, Fig. 10(a) shows the calculated dispersion curves for an SOI strip nanowire with e.g. $h_{co}=220$ nm. Figures 10(b)–10(d) shows the simulated light propagation in the designed ADCs when choosing different core widths for the bus waveguide. It can be seen that an efficient mode excitation is achieved from the TM_0 mode in the narrow access-waveguide to the desired higher-order mode in the wide bus-waveguide, with very little power left in the access waveguide. When these ADCs are cascaded by inserting an adiabatic taper between two adjacent stages, a mode multiplexer with N mode-channels is realized as shown in Fig. 10(e) [51,86].

Figure 11(a) shows the fabricated PIC including a mode multiplexer (with input ports I_1–I_4), and a mode demultiplexer (with output ports O_1–O_4), which is used to characterize the mode convert-(de)multiplexer. Figures 11(b)–11(e) show the measured transmission responses at all output ports O_1, O_2, O_3, and O_4 when light is input from port I_1, I_2, I_3, and I_4 respectively. It can be seen that one has the maximal output from the jth input port to the jth output port as desired. The fabricated device has low excess loss (<0.5 dB) and low crosstalk (<-20 dB) over a broad band around the central wavelength. The total insertion loss of about 12–13 dB is mainly from the butt-coupling loss between the fiber and the chip, which can be reduced by introducing grating couplers or inversed tapers. The ADC-based mode multiplexer can also be further extended to deal with the modes for both polarizations so that the link capacity is doubled. Figure 12(a) shows the proposed ADC-based (de)multiplexer for both polarizations [91]. Here the TE_0 and TM_0 modes combined/separated by using a PBS based on a three-waveguide coupler [25] while the high-order modes (TE_1, TE_2, TE_3, TM_1, TM_2, and TM_3) are (de)multiplexed by using six cascaded ADCs. Figure 12(b) shows the fabricated 8-channel hybrid multiplexer. The present hybrid (de)multiplexer works well (with low crosstalk and low loss) over a broad wavelength band [91]. The performance can be improved by introducing polarizers to filter out the polarization crosstalks [92]. The broad-band performance makes the ADC-based mode multiplexers available for WDM systems so that it is possible to realize the hybrid multiplexing technology combining WDM and MDM.

3 PICs with ADCs

3.1 Hybrid (de)multiplexer enabling PDM and WDM

A polarization-diversity circuit including PBSs and

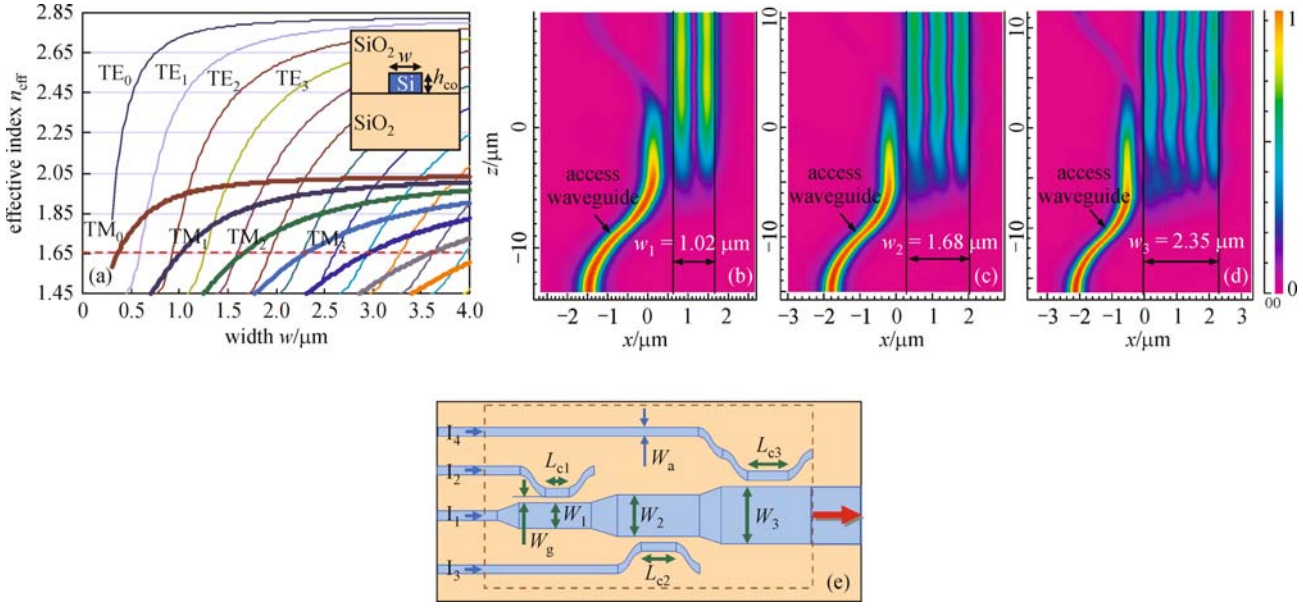

Fig. 10 (a) Calculated effective indices of the guided-modes in an SOI strip nanowire with $h_{co}=220$ nm; the FDTD simulated light propagation in the designed ith stage ADC with (b) $i=1$, (c) $i=2$, and (d) $i=3$; (e) schematic configuration of the mode converter-multiplexer with 4 channels [86]

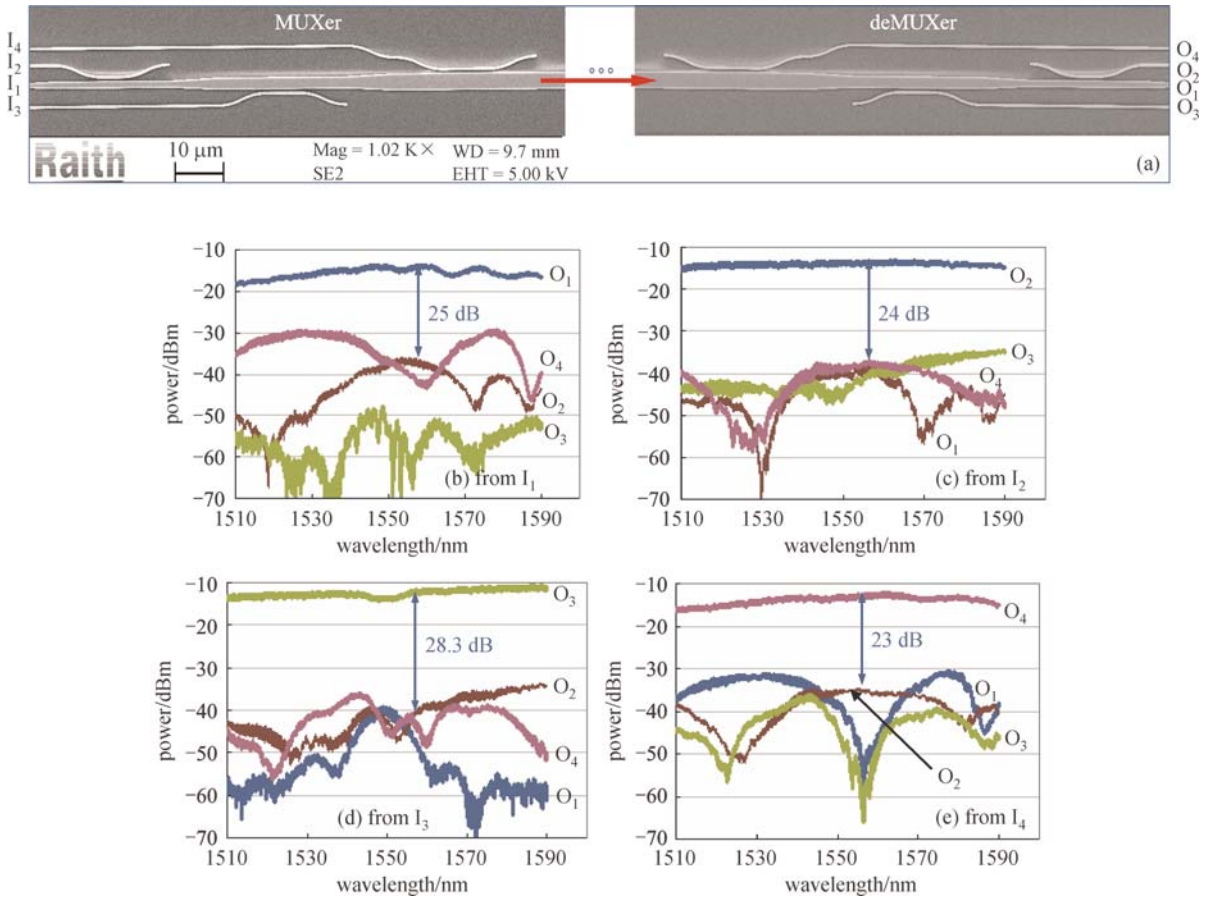

Fig. 11 (a) SEM picture for the 4×1 mode multiplexer and 1×4 mode demultiplexer integrated on the same chip; measured responses at output ports (O_1, O_2, O_3, and O_4) when light is input from the port of (b) I_1, (c) I_2, (d) I_3, and (e) I_4 [86]

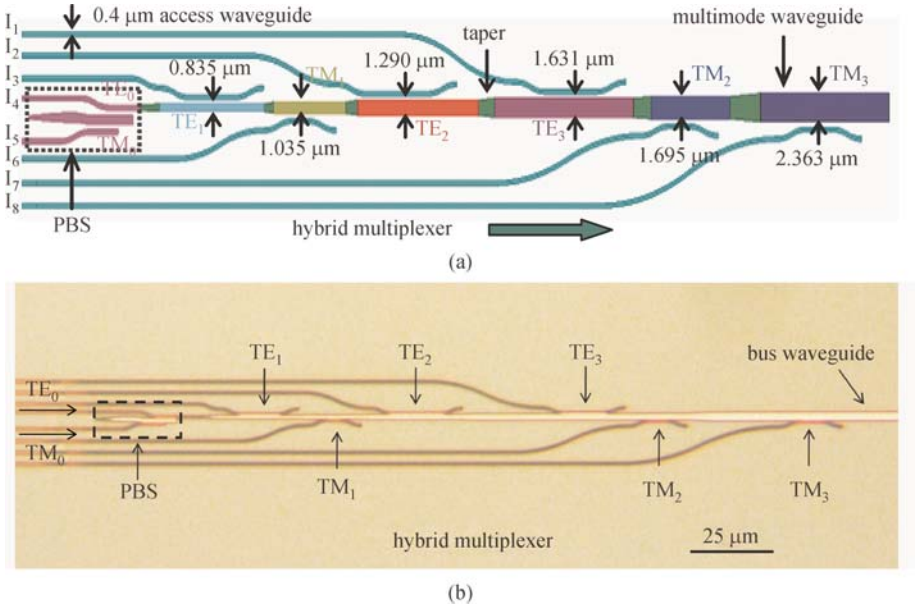

Fig. 12 (a) 8-channel hybrid multiplexer enabling mode- and polarization-division-(de)multiplexing simultaneously; (b) the fabricated 8-channel hybrid multiplexer [91]

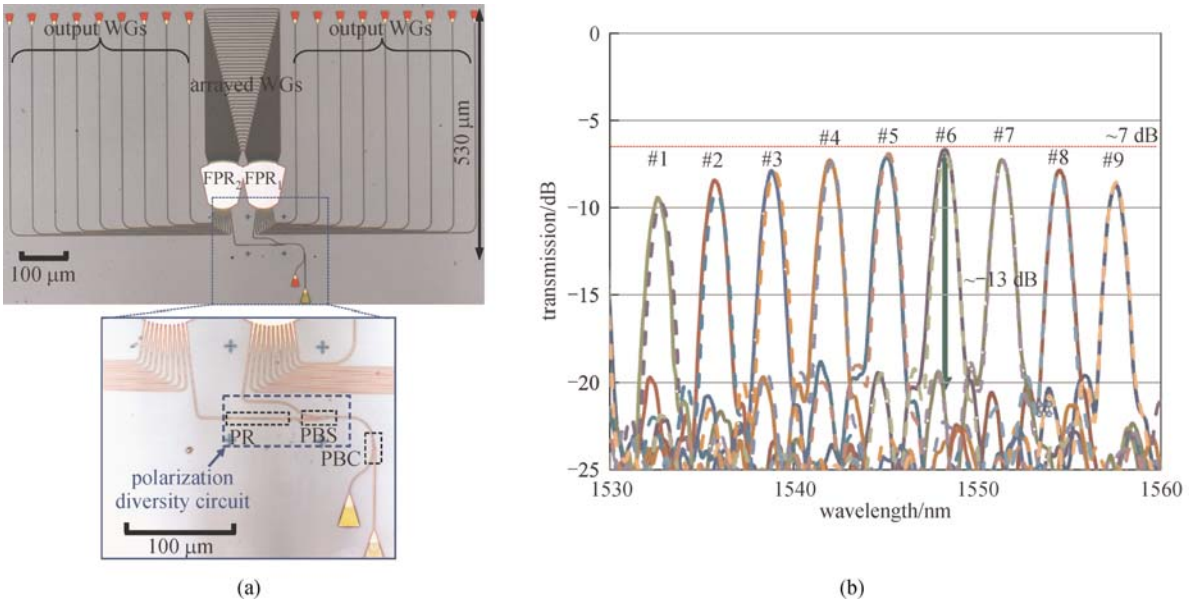

Fig. 13 A 18-channel PDM-WDM hybrid (de)multiplexer (a) and the measurement responses of all the channels (b)

polarization rotators (PRs) enables polarization-insensitive PICs as well as PICs working for dual-polarizations. For example, the polarization-diversity circuit can be realized by including a PBS based on a bent ADC [40,41], and a PR based on a SOI nanowire with a cut corner [93]. When a polarization-diversity circuit working with an arrayed waveguide grating (AWG), it is possible to realize the hybrid (de)multiplexing technology combining WDM as well as PDM, as shown in Fig. 13(a). The bi-directional AWG has $N+1$ access optical waveguides at both sides. The input $2N$ channels of optical signals are separated into the TE-polarization group and the TM-polarization group by a broadband PBS. Each group has N wavelength channels (λ_1, λ_2,..., λ_N). The TM-polarization group is then rotated and converted to be TE polarization by using a broadband PR. These two groups of signals are then input to the two input waveguides of the bi-directional AWG and then demultiplexed respectively by the bi-directional AWG. In this way, there are $2N$ output waveguides to receive $2N$ channels carried by N wavelengths (λ_1, λ_2,..., λ_N) and two polarizations (TE and TM), respectively. Figure 13(b) shows the measured spectral responses for the whole structure including a polarization beam combiner (PBC), PBS, PR, and bi-directional AWG. Here both the PBC and PBS are based on a bent ADC. The solid curves and the dashed curves are for the channels output from the ports at the right side (TM polarization) as well as at the left side (TE polarization). It can be seen that these two groups of channels are aligned very well with nearly zero polarization dependent wavelength (PDλ), which is guaranteed intrinsically by such a bi-directional AWG working as two AWGs sharing the identical dispersion waveguide grating.

3.2 Hybrid (de)multiplexer enabling MDM and WDM

Mode demultiplexer based on cascaded ADCs is broadband and thus it is WDM-compatible. Therefore, it is possible to enable the MDM and WDM simultaneously [94] when a mode demultiplexer works with multiple AWG demultiplexers, as shown in Fig. 14(a). In the present case, there are 64 channels to be demultiplexed in total by using a 1×4 ADC-based mode demultiplexer and four identical 16-channel AWGs with a channel spacing of 3.2 nm. Figure 14(b) show the measured normalized spectral responses for all the channels of the fabricated hybrid demultiplexer when light is launched at input port I_1, I_2, I_3, and I_4, respectively. From these figures, it can be seen that the crosstalk at the output ports of AWG #j ($j\neq i$) from by the undesired mode coupling is about −16~−25 dB. The spectral responses of the wavelength-channels are similar to those of a discrete AWG demultiplexer on the same chip, which benefits from the broadband performance of the ADC-based mode demultiplexer. It proves that the ADC-based mode demultiplexer work together with AWG demultiplexers very well. A simplified version for hybrid MDM-WDM (de)multiplexer can be realized by introducing bi-directional $N\times N$ AWGs which can work equally as two $1\times N$ AWG. In this way, less AWGs are indeed and the chip become more compact [95].

4 Conclusions

In summary, we have reviewed our recent work on silicon-based ADCs, which can be constructed with two or three non-identical waveguides in the coupling region. Silicon-

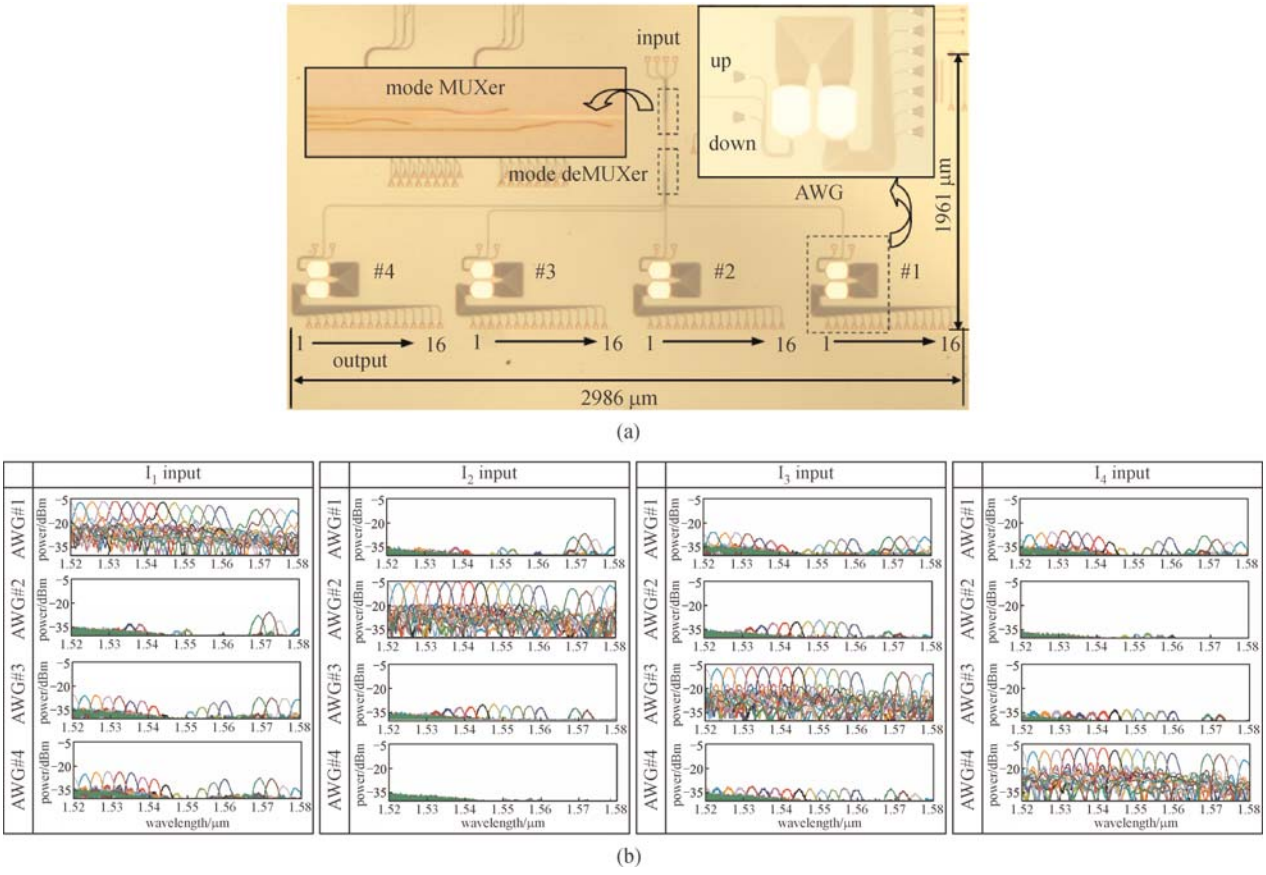

Fig. 14 A 64-channel MDM-WDM hybrid multiplexer (a) and the measurement results (b) [94]

based ADCs have some unique performances and applications because of the ultra-high index-contrast and ultra-small cross section of the SOI nanophotonic waveguides. A basic design rule for ADCs is the so-called phase-matching condition. The waveguide dimensions should be chosen optimally to make the phase-matching condition satisfied so that the desired mode coupling happens efficiently. In this paper, we have discussed the applications of ADCs for power splitting, polarization-beam splitting, as well as mode demultiplexing. For example, an ADC with two bent waveguides has been used successfully to achieve sufficient coupling for cascaded microring filters as a better option than the conventional MMI couplers or straight DCs. This kind of bent coupler can be also used to realize an ultra-short PBS because the phase matching condition can be satisfied for one polarization only due to the high birefringence of SOI nanowires. An ADC can be also formed by introducing different types of optical waveguides for the coupling region. For example, the regular SOI nanowire can be used as one of the coupling waveguides while the other waveguide in the coupling region can be made of some special optical waveguide like silicon nano-slot waveguide, silicon hybrid plasmonics waveguides, etc. In this case, the two waveguides can be designed optimally to satisfy the phase-matching condition for only one polarization since they have different birefringence. The strong polarization dependence makes it possible to realize ultra-short PBSs. Another type of ADC is formed by using two waveguides with different core widths, in which case it is to couple the fundamental mode in the narrow optical waveguide to the higher-order mode in the wide optical waveguide by optimizing their widths to make their effective indices equal. This kind of coupling is also polarization dependent, which provides an option to realize a compact PBS. More importantly, this ADC enabling the efficient coupling between the fundamental mode in a narrow waveguide and the higher-order mode in a wide waveguide can be used to realize mode (de)multiplexing, which is very attractive for realizing the mode (de)multiplexer used in mode-division-multiplexed systems. Finally the ADCs in this paper are SOI-compatible so that it is easy and convenient to monolithically integrate these power splitters, PBSs as well as mode (de)multiplexers based on ADCs with other elements on the same chip, like hybrid WDM-PDM (de)multiplexers, and hybrid WDM-MDM (de)multiplexers.

Acknowledgements We thank Dr. Jian Wang, Dr. Pengxin Chen, Dr. Xiaowei Guan, Dr. Fei Lou, Prof. Lech Wosinski, Dr. Di Liang, Prof. John

Bowers, Dr. Yaocheng Shi, Prof. Sailing He, et al for their contributions and the support from the National Natural Science Foundation of China (NSFC) (Grant Nos. 11374263, 6141101056, 61422510), the Doctoral Fund of Ministry of Education of China (No. 20120101110094), and the Fundamental Research Funds for the Central Universities.

References

1. Fukuda H, Yamada K, Tsuchizawa T, Watanabe T, Shinojima H, Itabashi S. Ultrasmall polarization splitter based on silicon wire waveguides. Optics Express, 2006, 14(25): 12401–12408
2. Shi Y, Anand S, He S. Design of a polarization insensitive triplexer using directional couplers based on submicron silicon Rib waveguides. Journal of Lightwave Technology, 2009, 27(11): 1443–1447
3. Okamoto K. Fundamentals of Optical Waveguides.New York: Academic Press, 2010
4. Haus H A, Huang W P, Kawakami S, Whitaker N. Coupled-mode theory of optical waveguides. Journal of Lightwave Technology, 1987, 5(1): 16–23
5. Wagner R E, Cheng J. Electrically controlled optical switch for multimode fiber applications. Applied Optics, 1980, 19(17): 2921–2925
6. Schmidt R V, Alferness R C. Directional coupler switches, modulators, and filters using alternating Δb techniques. IEEE Transactions on Circuits and Systems, 1979, 26(12): 1099–1108
7. Kogelnik H, Schmidt R V. Switched directional couplers with alternating Δb. IEEE Journal of Quantum Electronics, 1976, 12(7): 396–401
8. Paniccia M J. A perfect marriage: optics and silicon. Optik & Photonik, 2011, 6(2): 34–38
9. Bogaerts W, Selvaraja S K, Dumon P, Brouckaert J, De Vos K, Van Thourhout D, Baets R. Silicon-on-insulator spectral filters fabricated with CMOS technology. IEEE Journal of Selected Topics in Quantum Electronics, 2010, 16(1): 33–44
10. Bogaerts W, Dumon P, Van Thourhout D, Taillaert D, Jaenen P, Wouters J, Beckx S, Wiaux V, Baets R. Compact wavelength-selective functions in silicon-on-insulator photonic wires. IEEE Journal of Selected Topics in Quantum Electronics, 2006, 12(6): 1394–1401
11. Sasaki K, Ohno F, Motegi A, Baba T. Arrayed waveguide grating of 70×60 μm^2 size based on Si photonic wire waveguides. Electronics Letters, 2005, 41(14): 801–802
12. Bogaerts W, Dumon P, Van Thourhout D, Taillaert D, Jaenen P, Wouter J, Beckx S, Wiaux V, Baets R G. Compact wavelength-selective functions in silicon-on-insulator photonic wires. IEEE Journal of Selected Topics in Quantum Electronics, 2006, 12(6): 1394–1401
13. Soltani M, Yegnanarayanan S, Adibi A. Ultra-high Q planar silicon microdisk resonators for chip-scale silicon photonics. Optics Express, 2007, 15(8): 4694–4704
14. Li C, Zhou L, Poon A W. Silicon microring carrier-injection-based modulators/switches with tunable extinction ratios and OR-logic switching by using waveguide cross-coupling. Optics Express, 2007, 15(8): 5069–5076
15. Rong H, Jones R, Liu A, Cohen O, Hak D, Fang A, Paniccia M. A continuous-wave Raman silicon laser. Nature, 2005, 433(7027): 725–728
16. Xu Q, Schmidt B, Pradhan S, Lipson M. Micrometre-scale silicon electro-optic modulator. Nature, 2005, 435(7040): 325–327
17. Barrios C A, Almeida V R, Panepucci R, Lipson M. Electrooptic modulation of silicon-on-insulator submicrometer-size waveguide devices. Journal of Lightwave Technology, 2003, 21(10): 2332–2339
18. Tang Y, Chen H W, Jain S, Peters J D, Westergren U, Bowers J E. 50 Gb/s hybrid silicon traveling-wave electroabsorption modulator. Optics Express, 2011, 19(7): 5811–5816
19. Dai D, Liu L, Wosinski L, He S. Design and fabrication of ultra-small overlapped AWG demultiplexer based on α-SOI nanowire waveguides. Electronics Letters, 2006, 42(7): 400–402
20. Fukuda H, Yamada K, Tsuchizawa T, Watanabe T, Shinojima H, Itabashi S. Silicon photonic circuit with polarization diversity. Optics Express, 2008, 16(7): 4872–4880
21. Vermeulen D, Van Acoleyen K, Ghosh S, Selvaraja S, De Cort W, Yebo N, Hallynck E, De Vos K, Debackere P, Dumon P, Bogaerts W, Roelkens G, Van Thourhout D, Baets R. Efficient tapering to the fundamental quasi-TM mode in asymmetrical waveguides. In: Proceedings of European Conference on Integrated Optics (ECIO), United Kingdom, 2010. Paper Wep16
22. Dai D, Bowers J E. Novel concept for ultracompact polarization splitter-rotator based on silicon nanowires. Optics Express, 2011, 19 (11): 10940–10949
23. Dai D, Bauters J, Bowers J E. Passive technologies for future large-scale photonic integrated circuits on silicon: polarization handling, light non-reciprocity and loss reduction. Light, Science & Applications, 2012, 1(3): e1
24. Dai D, Liu L, Gao S, Xu D, He S. Polarization management for silicon photonic integrated circuits. Laser & Photonics Reviews, 2013, 7(3): 303–328
25. Augustin L M, Van der Tol J J G M, Hanfoug R, de Laat W J M, Van de Moosdijk M J E, Van Dijk P W L, Oei Y, Smit M K. A single etch-step fabrication-tolerant polarization splitter. Journal of Lightwave Technology, 2007, 25(3): 740–746
26. Liang T K, Tsang H K. Integrated polarization beam splitter in high index contrast silicon-on-insulator waveguides. IEEE Photonics Technology Letters, 2005, 17(2): 393–395
27. Augustin L M, Hanfoug R, Van der Tol J, de Laat W J M, Smit M K. A compact integrated polarization splitter/converter in InGaAsP-InP. IEEE Photonics Technology Letters, 2007, 19(17): 1286–1288
28. Hong J M, Ryu H H, Park S R, Jeong J W, Gol L S, Lee E H, Park S G, Woo D, Kim S O B H. Design and fabrication of a significantly shortened multimode interference coupler for polarization splitter application. IEEE Photonics Technology Letters, 2003, 15(1): 72–74
29. Jiao Y, Dai D, Shi Y, He S. Shortened polarization beam splitters with two cascaded multimode interference sections. IEEE Photonics Technology Letters, 2009, 21(20): 1538–1540
30. Tu Z, Huang Y W, Yi H X, Wang X J, Li Y P, Li L, Hu W W.A compact SOI polarization beam splitter based on multimode interference coupler. Proceedings of SPIE-The International Society for Optical Engineering, 2011, 8307(1):1–6
31. Yang B K, Shin S Y, Zhang D. Ultrashort polarization splitter using

two-mode interference in silicon photonic wires. IEEE Photonics Technology Letters, 2009, 21(7): 432–434
32. Kiyat I, Aydinli A, Dagli N. A compact silicon-on-insulator polarization splitter. IEEE Photonics Technology Letters, 2005, 17 (1): 100–102
33. Xiao J, Liu X, Sun X. Design of a compact polarization splitter in horizontal multiple-slotted waveguide structures. Japanese Journal of Applied Physics, 2008, 47(5R): 3748–3754
34. Tu X, Ang S S N, Chew A B, Teng J, Mei T. An ultracompact directional coupler based on gaas cross-slot waveguide. IEEE Photonics Technology Letters, 2010, 22(17): 1324–1326
35. Yamazaki T, Aono H, Yamauchi J, Nakano H. Coupled waveguide polarization splitter with slightly different core widths. Journal of Lightwave Technology, 2008, 26(21): 3528–3533
36. Yue Y, Zhang L, Yang J Y, Beausoleil R G, Willner A E. Silicon-on-insulator polarization splitter using two horizontally slotted waveguides. Optics Letters, 2010, 35(9): 1364–1366
37. Shi Y, Dai D, He S. Proposal for an ultracompact polarization-beam splitter based on a photonic-crystal-assisted multimode interference coupler. IEEE Photonics Technology Letters, 2007, 19(11): 825–827
38. Ao X, Liu L, Wosinski L, He S. Polarization beam splitter based on a two-dimensional photonic crystal of pillar type. Applied Physics Letters, 2006, 89(17): 171115
39. Dai D. Silicon polarization beam splitter based on an asymmetrical evanescent coupling system with three optical waveguides. Journal of Lightwave Technology, 2012, 30(20): 3281–3287
40. Dai D, Bowers J E. Novel ultra-short and ultra-broadband polarization beam splitter based on a bent directional coupler. Optics Express, 2011, 19(19): 18614–18620
41. Wang J, Liang D, Tang Y, Dai D, Bowers J E. Realization of an ultra-short silicon polarization beam splitter with an asymmetrical bent directional coupler. Optics Letters, 2013, 38(1): 4–6
42. Komatsu M A, Saitoh K, Koshiba M. Design of miniaturized silicon wire and slot waveguide polarization splitter based on a resonant tunneling. Optics Express, 2009, 17(21): 19225–19233
43. Dai D, Wang Z, Bowers J E. Ultrashort broadband polarization beam splitter based on an asymmetrical directional coupler. Optics Letters, 2011, 36(13): 2590–2592
44. Lin S, Hu J, Crozier K B. Ultracompact, broadband slot waveguide polarization splitter. Applied Physics Letters, 2011, 98(15): 151101
45. Lou F, Dai D, Wosinski L. Ultracompact polarization beam splitter based on a dielectric-hybrid plasmonic-dielectric coupler. Optics Letters, 2012, 37(16): 3372–3374
46. Chee J, Zhu S, Lo G Q. CMOS compatible polarization splitter using hybrid plasmonic waveguide. Optics Express, 2012, 20(23): 25345–25355
47. Guan X, Wu H, Shi Y, Wosinski L, Dai D. Ultracompact and broadband polarization beam splitter utilizing the evanescent coupling between a hybrid plasmonic waveguide and a silicon nanowire. Optics Letters, 2013, 38(16): 3005–3008
48. Almeida V R, Xu Q, Barrios C A, Lipson M. Guiding and confining light in void nanostructure. Optics Letters, 2004, 29(11): 1209–1211
49. Dai D, He S. A silicon-based hybrid plasmonic waveguide with a metal cap for a nano-scale light confinement. Optics Express, 2009, 17(19): 16646–16653
50. Song Y, Wang J, Li Q, Yan M, Qiu M. Broadband coupler between silicon waveguide and hybrid plasmonic waveguide. Optics Express, 2010, 18(12): 13173–13179
51. Dai D. Silicon mode-(de) multiplexer for a hybrid multiplexing system to achieve ultrahigh capacity photonic networks-on-chip with a single-wavelength-carrier light. In: Proceedings of Communications And Photonics Conference (ACP), IEEE, 2012, 1–3
52. Little B E, Chu S T, Absil P P, Hryniewicz J V, Johnson F G, Seiferth F, Gill D, Van V, King O, Trakalo M. Very high-order microring resonator filters for WDM applications. IEEE Photonics Technology Letters, 2004, 16(10): 2263–2265
53. Luo X, Song J, Feng S, Poon A W, Liow T Y, Yu M, Lo G Q, Kwong D L. Silicon high-order coupled-microring-based electro-optical switches for on-chip optical interconnects. IEEE Photonics Technology Letters, 2012, 24(10): 821–823
54. Tobing L Y M, Dumon P, Baets R, Chin M K. Boxlike filter response based on complementary photonic bandgaps in two-dimensional microresonator arrays. Optics Letters, 2008, 33(21): 2512–2514
55. Melloni A. Synthesis of a parallel-coupled ring-resonator filter. Optics Letters, 2001, 26(12): 917–919
56. Little B E, Chu S T, Haus H A, Foresi J, Laine J P. Microring resonator channel dropping filters. Journal of Lightwave Technology, 1997, 15(6): 998–1005
57. Xia F, Rooks M, Sekaric L, Vlasov Y. Ultra-compact high order ring resonator filters using submicron silicon photonic wires for on-chip optical interconnects. Optics Express, 2007, 15(19): 11934–11941
58. Bachmann M, Besse P A, Melchior H. General self-imaging properties in $N \times N$ multimode interference couplers including phase relations. Applied Optics, 1994, 33(18): 3905–3911
59. Chen P, Chen S, Guan X, Shi Y, Dai D. High-order microring resonators with bent couplers for a box-like filter response. Optics Letters, 2014, 39(21): 6304–6307
60. Morino H, Maruyama T, Iiyama K. Reduction of wavelength dependence of coupling characteristics using si optical waveguide curved directional coupler. Journal of Lightwave Technology, 2014, 32(12): 2188–2192
61. Xia F, Sekaric L, Vlasov Y A. Mode conversion losses in silicon-on-insulator photonic wire based racetrack resonators. Optics Express, 2006, 14(9): 3872–3886
62. Soldano L B, de Vreede A I, Smit M K, Verbeek B H, Metaal E G, Groen F H. Mach-Zehnder interferometer polarization splitter in InGaAsP/InP. IEEE Photonics Technology Letters, 1994, 6(3): 402–405
63. Tang Y, Dai D, He S. Proposal for a grating waveguide serving as both a polarization splitter and an efficient coupler for silicon-on-insulator nanophotonic circuits. IEEE Photonics Technology Letters, 2009, 21(4): 242–244
64. Alam M Z, Meier J, Aitchison J S, Mojahedi M.Super mode propagation in low index medium. In: Proceeding of Photonic Applications Systems Technologies Conference, Optical Society of America, 2007, Jthd112
65. Oulton R F, Sorger V J, Genov D A, Pile D F P, Zhang X. A hybrid plasmonic waveguide for subwavelength confinement and long-range propagation. Nature Photonics, 2008, 2(8): 496–500
66. Oulton R F, Sorger V J, Zentgraf T, Ma R M, Gladden C, Dai L,

Bartal G, Zhang X. Plasmon lasers at deep subwavelength scale. Nature, 2009, 461(7264): 629–632

67. Fujii M, Leuthold J, Freude W. Dispersion relation and loss of subwavelength confined mode oof metal-dielectric-gap optical waveguides. IEEE Photonics Technology Letters, 2009, 21(6): 362–364
68. Sorin W V, Kim B Y, Shaw H J. Highly selective evanescent modal filter for two-mode optical fibers. Optics Letters, 1986, 11(9): 581–583
69. Li A, Chen X, Amin A A, Shieh W. Fused fiber mode couplers for few-mode transmission. IEEE Photonics Technology Letters, 2012, 24(21): 1953–1956
70. Fontaine N K, Doerr C R, Mestre M A, Ryf R, Winzer P, Buhl L, Sun Y, Jiang X, Lingle R.Space-division multiplexing and all-optical MIMO demultiplexing using a photonic integrated circuit. In: Proceeding of Optical Fiber Communication Conference, Optical Society of America, 2012, PDP5B. 1
71. Wohlfeil B, Stamatiadis C, Zimmermann L, Petermann K.Compact fiber grating coupler on SOI for coupling of higher order fiber modes. In: Proceeding of Optical Fiber Communication Conference, Optical Society of America, 2013, OTh1B. 2
72. Ding Y, Ou H, Xu J, Peucheret C. Silicon photonic integrated circuit mode multiplexer. IEEE Photonics Technology Letters, 2013, 25(7): 648–651
73. Koonen A M J, Chen H, Van den Boom H P A, Raz O. Silicon photonic integrated mode multiplexer and demultiplexer. IEEE Photonics Technology Letters, 2012, 24(21): 1961–1964
74. Uematsu T, Ishizaka Y, Kawaguchi Y, Saitoh K, Koshiba M. Design of a compact two-mode multi/demultiplexer consisting of multi-mode interference waveguides and a wavelength insensitive phase shifter for mode-division multiplexing transmission. Journal of Lightwave Technology, 2012, 30(15): 2421–2426
75. Greenberg M, Orenstein M. Multimode add-drop multiplexing by adiabatic linearly tapered coupling. Optics Express, 2005, 13(23): 9381–9387
76. Greenberg M Y, Orenstein M.Mode add drop for optical interconnects based on adiabatic high order mode couplers. In: Proceedings of Quantum Electronics and Laser Science Conference, Optical Society of America, 2005, JTuC55
77. Xing J, Li Z, Xiao X, Yu J, Yu Y. Two-mode multiplexer and demultiplexer based on adiabatic couplers. Optics Letters, 2013, 38 (17): 3468–3470
78. Love J D, Vance R W C, Joblin A. Asymmetric, adiabatic multipronged planar splitters. Optical and Quantum Electronics, 1996, 28(4): 353–369
79. Lee B T, Shin S Y. Mode-order converter in a multimode waveguide. Optics Letters, 2003, 28(18): 1660–1662
80. Low A L Y, Yong Y S, You A H, Chien S F, Teo C F. A five-order mode converter for multimode waveguide. IEEE Photonics Technology Letters, 2004, 16(7): 1673–1675
81. Riesen N, Love J D. Spatial mode-division-multiplexing of few-mode fiber. In: Proceedings of European Conference and Exhibition on Optical Communication, Optical Society of America, 2012, P2. 14
82. Riesen N, Love J D. Design of mode-sorting asymmetric Y-junctions. Applied Optics, 2012, 51(15): 2778–2783
83. Driscoll J B, Grote R R, Souhan B, Dadap J I, Lu M, Osgood R M. Asymmetric Y junctions in silicon waveguides for on-chip mode-division multiplexing. Optics Letters, 2013, 38(11): 1854–1856
84. Chen W, Wang P, Yang J. Mode multi/demultiplexer based on cascaded asymmetric Y-junctions. Optics Express, 2013, 21(21): 25113–25119
85. Bagheri S, Green W. Silicon-on-insulator mode-selective add-drop unit for on-chip mode-division multiplexing. In: Proceedings of 2009 6th IEEE International Conference on Group IV Photonics, 2009
86. Dai D, Wang J, Shi Y. Silicon mode (de)multiplexer enabling high capacity photonic networks-on-chip with a single-wavelength-carrier light. Optics Letters, 2013, 38(9): 1422–1424
87. Hanzawa N, Saitoh K, Sakamoto T, Matsui T, Tsujikawa K, Koshiba M, Yamamoto F. Two-mode PLC-based mode multi/demultiplexer for mode and wavelength division multiplexed transmission. Optics Express, 2013, 21(22): 25752–25760
88. Qiu H, Yu H, Hu T, Jiang G, Shao H, Yu P, Yang J, Jiang X. Silicon mode multi/demultiplexer based on multimode grating-assisted couplers. Optics Express, 2013, 21(15): 17904–17911
89. Luo L W, Ophir N, Chen C, Gabrielli L H, Poitras C B, Bergman K, Lipson M. Simultaneous mode and wavelength division multiplexing on-chip. arXiv preprint arXiv:1306.2378, 2013
90. Ding Y, Xu J, Da Ros F, Huang B, Ou H, Peucheret C. On-chip two-mode division multiplexing using tapered directional coupler-based mode multiplexer and demultiplexer. Optics Express, 2013, 21(8): 10376–10382
91. Wang J, He S, Dai D. On-chip silicon 8-channel hybrid (de) multiplexer enabling simultaneous mode-and polarization-division-multiplexing. Laser & Photonics Reviews, 2014, 8(2): L18–L22
92. Wang J, Chen P, Chen S, Shi Y, Dai D. Improved 8-channel silicon mode demultiplexer with grating polarizers. Optics Express, 2014, 22(11): 12799–12807
93. Wang Z, Dai D. Ultrasmall Si-nanowire-based polarization rotator. JOSA B, 2008, 25(5): 747–753
94. Wang J, Chen S, Dai D. Silicon hybrid demultiplexer with 64 channels for wavelength/mode-division multiplexed on-chip optical interconnects. Optics Letters, 2014, 39(24): 6993–6996
95. Dai D, Wang J, Chen S, Wang S, He S. Monolithically integrated 64-channel silicon hybrid demultiplexer enabling simultaneous wavelength-and mode-division-multiplexing. Laser & Photonics Reviews, 2015, 9(3): 339–344

Daoxin Dai received the B. Eng. degree from the Department of Optical Engineering, Zhejiang University (China), and the Ph.D. degree from Royal Institute of Technology (Sweden), in 2000 and 2005, respectively. He joined Zhejiang University as an assistant professor in 2005 and became an associate professor in 2007, a full professor in 2011. He visited the Chinese University of Hong Kong in 2005, and Inha University (Korea) in 2007. Dr. Dai worked at the University of California, Santa Barbara as a visiting scholar from the end of 2008 until 2011. His current research interests

include silicon nanophotonics for optical interconnections and optical sensing. He has published about 130 refereed international journals papers (including 8 invited review papers), and holds 11 patents. Dr. Dai has been invited to give more than 30 invited talks and served as the program committee member or session chair for some top international conferences (including OFC 2013–2015). He is serving as the Associate Editor of the Journals of "*IEEE Photonics Technology Letters*", "*Optical and Quantum Electronics*" and "*Photonics Research*".

Shipeng Wang received the B.Eng. degree from the Department of Optical Engineering, Zhejiang University, Hangzhou, China, in 2014. He is currently working toward the Ph.D. degree in the same Department of Zhejiang University. His research interests include silicon nanophotonic integrated waveguides and the applications.